Research Article

Jun Wang, Linxiang Liu, Jianwei Jiang*

Investigation of the spectroelectrochemical behavior of quercetin isolated from *Zanthoxylum bungeanum*

https://doi.org/10.1515/chem-2021-0031
received July 16, 2020; accepted February 9, 2021

Abstract: Flavonoids are common bioactive components in plants. Quercetin is the most abundant flavonoid in the human diet, accounting for more than half of the total daily consumption of flavonoids. In this study, adsorption and electrocatalytic activities of quercetin isolated from *Zanthoxylum bungeanum* on an electrode was studied via homemade electrodes. An *in situ* UV-Visible thin-layer spectroelectrochemical method was used to study the electrochemical behavior of quercetin in detail and to explore its electrochemical reaction mechanism. This experiment proves that UV-Vis thin-layer spectroelectrochemistry is a feasible way for studying the electrochemical reaction mechanism of flavonoids in plants.

Keywords: flavonoids, spectroelectrochemistry, electrochemical reaction mechanism, *Zanthoxylum bungeanum*, quercetin

1 Introduction

Zanthoxylum bungeanum is a kind of plant resource with high edible and medicinal value [1,2]. The chemical components of *Z. bungeanum* mainly include volatile oils, alkaloids, amides, coumarins, and flavones. Flavonoids are a kind of common bioactive component in plants [3,4]. In recent years, quercetin, hyperoside, anisidine, arbutin, and rutin have been isolated from the pericarp of *Z. bungeanum* [5,6].

*** Corresponding author: Jianwei Jiang,** Department of Pharmacy, Cancer Hospital of the University of Chinese Academy of Sciences (Zhejiang Cancer Hospital), Hangzhou, Zhejiang 310022, China; Institute of Cancer and Basic Medicine (IBMC), Chinese Academy of Sciences, Hangzhou, Zhejiang 310022, China,
e-mail: swpru5v2@21cn.com
Jun Wang, Linxiang Liu: Department of Pharmacy, The Hospital of Zhejiang University, Hangzhou, Zhejiang 310027, China

Quercetin is the most abundant flavonoid in the human diet, accounting for more than half of the total daily consumption of flavonoids. Ionizing radiation can produce a large number of free radicals and cause a series of free radical reactions, including lipid peroxidation [7–9]. Excessive free radicals are harmful and can lead to changes in the cellular structure and the destruction of cellular functions, which may cause cancer, increased ageing, cardiovascular disease, and other health concerns. Quercetin can combine with Fe(III) and Mn(II) ions, and its role as an antioxidant may be achieved by affecting the internal balance of metal ions, thus changing their oxidation state in cells [10–13]. NO is a messenger molecule found in recent years, which is a part of many physiological activities. Excessive NO production in the brain can lead to neurodegenerative diseases. Quercetin can inhibit the production of NO in a dose-dependent manner and thus shows a preventive effect on neurodegenerative diseases. Furthermore, the incubation of 10 mg of quercetin with the HepG2 cell line can effectively inhibit the binding activity of nuclear factor kappa B and protect against injuries induced by H_2O_2 [14–16].

Electrochemical methods have been widely used for studying the antioxidation activity of natural antioxidants; in addition, these methods have been used for the analysis and detection of natural antioxidants [17–19]. The main research contents of electrochemical methods can be summarized as the electrochemical detection of flavonoids and the kinetic study of electrode processes. However, the evaluation of the antioxidant activity of natural antioxidants and the interaction between natural antioxidants and natural oxidants have also been reported [20,21]. Cyclic voltammetry, as a simple and fast electrochemical method, has been used by many researchers to detect antioxidants [22–24]. Differential pulse voltammetry, oscillopolarography, and flow injection amperometric methods have also been used in the analysis of natural antioxidants [25–27]. Choosing a suitable method is the key for improving detection sensitivity. By using electrochemical

theories and methods, the reversibility of a reaction can be obtained from the electrochemical data, and the apparent kinetic parameters, such as the number of electron transfers, rate constants, exchange current densities, and transfer coefficients, can be obtained; furthermore, the intermediate particles and products can be detected [28,29].

Spectroelectrochemistry is an interdisciplinary field developed in chronology. A simple electrochemical measurement technique can only obtain indirect information about the interfacial structure and reaction history of the electrode solution [30,31]. The main disadvantage of electrochemical techniques is that they only have pure electrochemical measurements and lack the characteristics of the electrode reaction molecules; thus, there is no useful information about reaction products or intermediates [32]. Spectroelectrochemistry is a method that combines spectroscopy and electrochemical methods to simultaneously measure an electrolytic cell. Generally, the spectroelectrochemical spectrum uses electrochemistry as the excitation signal, and the response of the system to the electrical excitation signal is monitored by the spectroscopic technology [33,34]. The two are closely combined to exert their respective advantages. In this way, a variety of information can be obtained at the same time, which provides a very powerful research method for studying the electrode process mechanism and electrode surface characteristics, along with identifying the intermediates of reaction processes, transient states, and product properties; moreover, certain electrochemical parameters can be measured [35,36].

It is often difficult to study the redox reaction of drugs *in vivo*. According to the research characteristics of medicinal chemistry, people often choose electrochemical techniques to study the electron transfer properties of drugs for simulating or assisting the exploration of the redox process of drugs *in vivo* [37,38]. Chemical reactions of drug molecules often occur in multiple steps, and the reaction mechanism is complex; therefore, it is difficult to accurately determine them by general methods [39–41]. UV-Vis spectroscopy has unique advantages in identifying reactive substances, especially the transient states and intermediates of the reaction. Therefore, UV-Vis spectroscopy can immediately provide considerable information about reactants, intermediates, and products, thereby making it a powerful method to study electrochemical reactions and mechanisms [42,43]. Many drug molecules have characteristic absorption in the ultraviolet-visible region, which makes it possible to study the properties of drug molecules by spectroelectrochemistry. The thin-layer spectroelectrochemical measurement requires a short electrolysis time, which makes it easy to control the directional electron transfer properties of drug molecules, and the drug distribution in the thin-layer solution is uniform [44,45]. Thin-layer spectroelectrochemistry can also be used to study the adsorption properties of drugs on electrode surfaces.

The purpose of this study is to enhance adsorption and electrocatalytic activities of quercetin on the electrode by using homemade electrodes and to use *in situ* UV-Visible thin-layer spectroelectrochemical methods to study the electrochemical behavior of quercetin in detail and explore its electrochemical reaction mechanism.

2 Experimental

All reagents were of analytical grade. Paraffin wax and graphite powder were spectrally pure, and other reagents were analytically pure. Quercetin was isolated from *Z. bungeanum* (inset of Figure 1). When designing a thin-layer electrochemical cell, to avoid modifying the sample cell of the spectrophotometer, a common cuvette was directly used as the cell body. The research electrode should be easily fixed and removed for grinding and cleaning before the experimental test.

To obtain the changes in the concentrations of reactants and products in the thin-layer liquid phase during the electrode reaction, the parallel incidence method was adopted, that is, the incident light was projected across the electrode surface in parallel with the electrode surface. For the light path of the Shimadzu UV-Vis 2550 spectrophotometer used in the experiment, the electrode

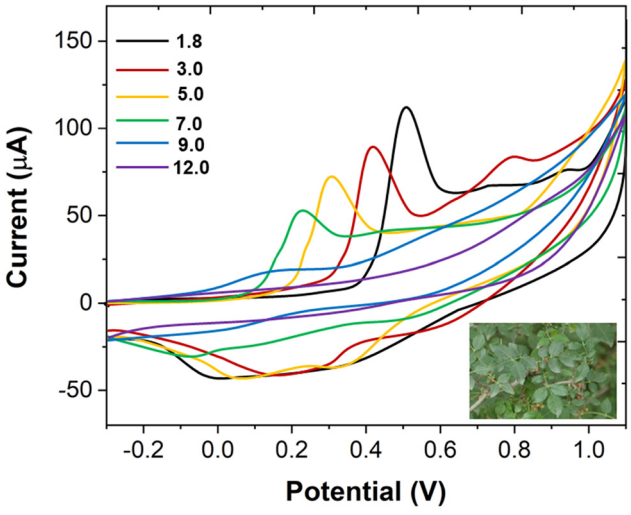

Figure 1: CV curves of quercetin in different pH values of B–R buffer solutions (0.1 M). Scan rate: 50 mV/s.

surface should be inserted vertically into the cuvette. A certain slit was formed by a gasket of a certain thickness at the upper and lower ends of the electrode plate, and another baffle was used in the cuvette. This slit formed a thin layer of electrolyte, and the thickness was the thickness of the gasket. The thickness of the thin pool could be adjusted by changing the thickness of the gasket.

A certain amount of quercetin stock solution was taken and diluted with a certain amount of buffer to obtain the required concentration of quercetin solution. A cuvette was filled with a certain amount of quercetin solution. The research electrode was inserted, and the thin cell was filled with solution to drive out air bubbles. The reference electrode and the platinum mesh auxiliary electrode were inserted, and a syringe was used to aspirate excess solution. The cuvette was inserted into the sample cell of the spectrophotometer, and leads of the three electrodes were led out of the test system. The quercetin was scanned by cyclic voltammetry and potentiostatic electrolysis, and the scanning spectrum and absorbance–time curve of the thin-layer cell solution were recorded.

Ethical approval: The conducted research is not related to either human or animal use.

3 Results and discussion

Figure 1 shows the large range of CV curves of quercetin in B–R buffer solution (0.1 M) at different pH values. It can be seen from the figure that with the increase in the pH value, redox peak potentials of quercetin are negatively shifted, and the peak current tends to be smaller. When the pH value reaches 12, almost no redox peak appears. When pH = 1.8, the system shows the best CV curve, with a good peak shape and large peak current. This behavior change may be caused by the hydrolysis of quercetin. Therefore, pH of 1.8 was selected for further study.

Figure 2 shows the repeated scanning of the UV-Vis spectrum of the solution in the thin-layer cell during the constant potential oxidation process that was within the potential range of the first oxidation peak. At the beginning of the scanning, there are two maximum absorption peaks at 369 and 255 nm, which were the characteristic absorption peaks of quercetin. The absorption band of the first long wavelength is mainly due to the transition between the highest occupied molecular orbital and the lowest unoccupied molecular orbital (HOMO–LUMO) [46].

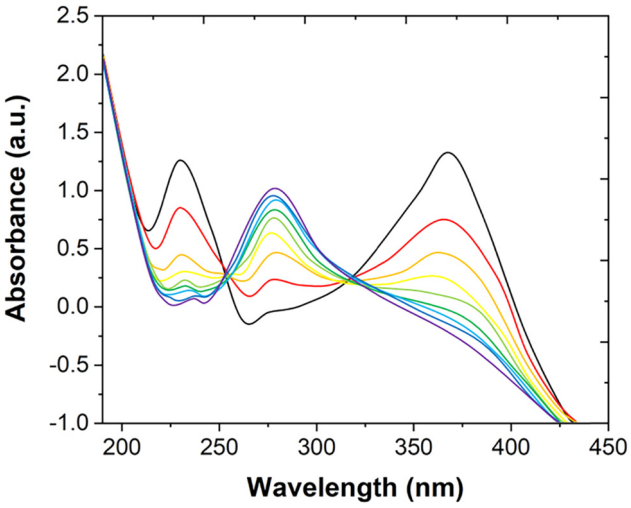

Figure 2: UV absorption spectrum of quercetin in a thin-layer cell during 0.47 V constant potential oxidation.

Due to the HOMO–LUMO conversion, the electron charge density of the B-ring shifts to the carbonyl bond of the C-ring [47]. Other transformations are the redistribution of charge throughout the molecule. For these compounds, the UV-Vis spectrum cannot distinguish the detailed structure of the molecule.

Figure 3 shows the change in the absorbance of quercetin on the quercetin electrode in the thin-layer cell under open-circuit conditions. As time passes, Abs_{369nm} starts to decrease from the initial maximum value to a limit value, indicating that quercetin has a certain adsorption on the electrode surface. If the concentration of quercetin is increased, the time needed to reach adsorption equilibrium will increase accordingly [48]. When the

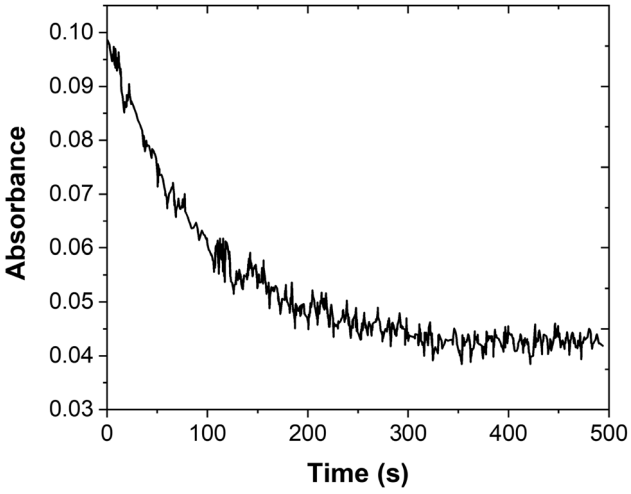

Figure 3: Absorbance time curve of quercetin in a thin-layer cell under the open-circuit condition.

electrode surface is replaced by a polyethylene plate, Abs_{369nm} did not change over time, indicating that quercetin adsorption is carried out on the electrode surface rather than on the polyethylene plate.

Figure 4 shows the *in situ* kinetic tests of quercetin and its oxidation products in the thin-layer cell at 369 and 293 nm, respectively. In the course of repeated EMF scanning, the absorbance of the thin-layer solution shows periodic changes at both wavelengths. During forward scanning, Abs_{369nm} decreases with time, while Abs_{293nm} increases, which corresponds to the decrease in the quercetin concentration and the increase in the product concentration. In the back sweep of potential, due to the opposite electrode process, the product is reduced, so the corresponding absorbance change is also opposite to that of the forward sweep. However, the amplitude of the change is smaller than that during forward scanning, especially in the case of a slow scan (Figure 4a). With the increase in the number of scanning cycles, the overall Abs_{369nm} shows a decreasing trend, while the overall Abs_{293nm} shows an increasing trend (Figure 4a and b). At the same time, Figure 4a and b clearly shows that not only quercetin is preadsorbed on the electrode surface before the power is turned on participating in the electron transfer reaction but also quercetin and its products in solution participate in the reaction through the preadsorption and subsequent desorption steps [49,50].

It is generally believed that for a quasi-reversible reaction, the reversibility of the system will decrease with the increasing scanning speed. Comparing Figure 4a and b, it can be seen that the studied reaction has high reversibility at high scanning speeds, which is contrary to the performance of typical quasi-reversible reactions [51,52]. When the scanning speed is fast enough (Figure 4c), Abs_{369nm} and Abs_{293nm} hardly change with the number of cycles, showing the properties of a nearly ideal reversible system.

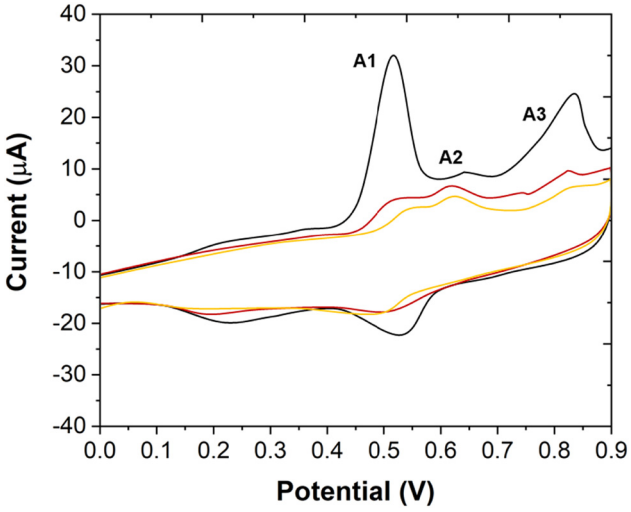

Figure 5: Cyclic voltammetric curves scanned between 0 and 0.9 V in 0.1 M B–R buffer solution. Scan rate: 50 mV/s.

Figure 5 shows the cyclic voltammetry curve obtained from a wide range of potential scans. A significant feature is that in the subsequent cycle, the oxidation peaks (except A2) and reduction peaks decrease significantly. A2 becomes the main oxidation peak. In addition, at least from the second cycle, the reactants of A2 did not come from the products of A1. It can also be seen that A3 is a composite peak. In the second cycle, there are two small peaks attributed to A3 in the potential range. In addition, the reduction peaks on the curve are all very wide composite peaks.

Figure 6a shows the absorbance time curve of the quercetin solution during cyclic potential scanning at a rate of 5 mV/s and in the range of 0–0.9 V. It can be seen that Abs_{369nm} decreases to a very small value in the first

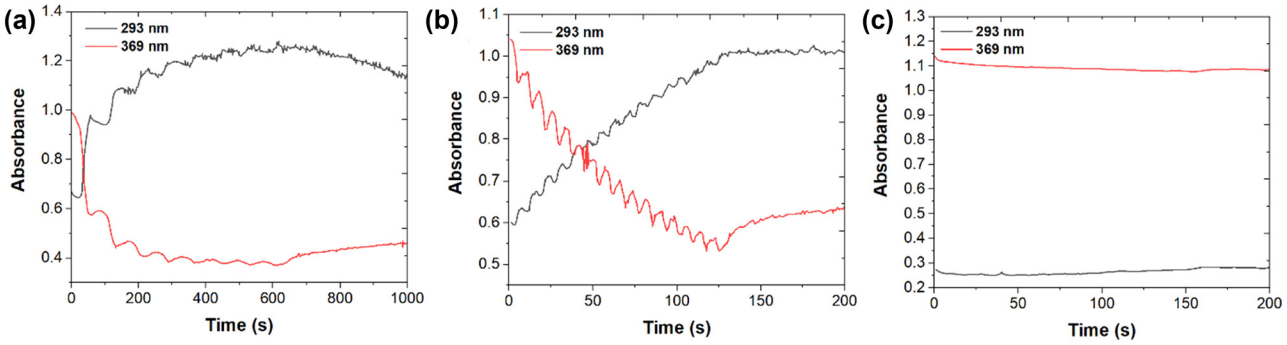

Figure 4: The dual wavelength absorbance time curve in the scanning process of quercetin cyclic potential: (a) scanning range: 0.3–0.5 V; quercetin concentration: 50 μm; pH = 1.8; scanning speed: 5 mV/s; number of cycles: 8. (b) Scanning speed: 50 mV/s; number of cycles: 16. (c) Scanning speed: 5 V/s; number of cycles: 1,500.

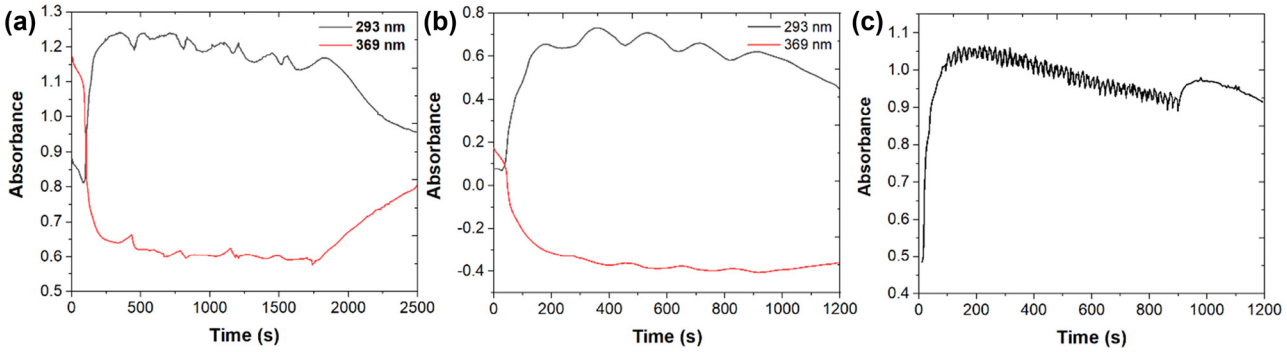

Figure 6: The dual wavelength absorbance time curve in the scanning process of quercetin cyclic potential: (a) scanning range: 0.0–0.9 V; quercetin concentration: 50 μm; pH = 1.8; scanning speed: 5 mV/s; number of cycle: 1. (b) Scanning speed: 10 mV/s; number of cycles: 5. (c) Scanning speed: 100 mV/s; number of cycles: 50.

forward scanning process, which makes the overall change in the subsequent scanning process small. Accordingly, Abs_{293nm} also reaches a high value in the first scan, which is similar to when the sweep speed is high. This result indicates that most quercetin in the thin-layer solution takes part in the reaction during the first forward scan, but the products in the solution are not significantly reduced back to their original forms during the reverse scan. It can be concluded that quercetin has been continuously adsorbed on the electrode surface to participate in the aforementioned oxidation reaction over the whole potential range of a 0.9 V sweep potential [53]. During the subsequent cycle, Abs_{293nm} shows periodic absorbance changes that are synchronized with the cyclic potential scanning, especially when the scanning speed is high (Figure 6b and c). However, it is remarkable that Abs_{293nm} decreases in the forward scan and increases in the reverse scan, which is the opposite of the periodicity of oxidation products and reduction products during cyclic scanning. The main reason for this phenomenon can be attributed to the influence of the added electrode potential on the adsorption of the product. In the back sweep of the potential, the product is driven by the interfacial electric field to desorb from the electrode surface into the solution and then adsorb to the electrode surface again during the forward sweep of the potential. During forward scanning, the electrode surface is covered by the continuous adsorption of the final product [54]. Figure 6a also shows that Abs_{369nm} shows a less obvious periodic change, which is opposite to that of Abs_{293nm}, indicating the competitive adsorption between the residual quercetin and final oxidation products on the electrode surface. In Figure 6a, we see a more complex periodic absorption wave, but it disappears when the scanning speed increases (Figure 6b and c). This complex wave appears simultaneously with the cyclic voltammetry peak, which is clearly related to the formation of oxidation products. When these products are formed on the electrode surface, they diffuse to the thin-layer solution due to supersaturation on the electrode surface. Then, with the positive change in potential, these products are adsorbed on the electrode surface, which results in the absorption wave. Because the adsorption and desorption process of oxidation products is relatively slow, this step is skipped when the scanning speed is fast.

4 Conclusion

In the homemade 0.2 mm-thick thin-layer electrochemical cell, the absorbance at two wavelengths expresses a good response to the electrochemical reaction process, thereby quickly and accurately showing the electrochemical reaction process. The oxidation behavior of quercetin is a chain reaction. The results show that quercetin adsorbed on the electrode surface and in the solution participates in the electrode reaction at the same time, and the electrode has strong adsorption behavior toward quercetin and its various oxidation products at high potentials. This experiment proves that UV-Vis thin-layer spectroelectrochemistry is a feasible way to study the electrochemical reaction mechanism of flavonoids in plants.

Funding information: This study was supported by Zhejiang scientific traditional Chinese medicine research fund (2016ZB020).

Author contributions: J. J.: conceptualization; J. J., J. W.: data curation; J. W. and J. J.: methodology; L. L.: formal analysis; J. W.: writing—original draft; J. J.: review and editing.

Conflict of interest: The authors declare no conflict of interest.

Data availability statement: The datasets generated during and/or analyzed during the current study are available from the corresponding author on reasonable request.

References

[1] Yan W, Yang X, Cao X, Long Y. Chemical constituents from Zanthoxylum bungeanum Dahongpao. Chin Tradit Pat Med. 2018;40(2):379–82.

[2] Hou X, Li S, Luo Q, Shen G, Wu H, Li M, et al. Discovery and identification of antimicrobial peptides in Sichuan pepper (Zanthoxylum bungeanum Maxim) seeds by peptidomics and bioinformatics. Appl Microbiol Biotechnol. 2019;103(5):2217–28.

[3] Zhang L-L, Xu S-S, Shi B-L, Wang H-Y, Liu L-Y, Zhong K, et al. Evaluation of the pungency intensity and time-related aspects of Chinese Zanthoxylum bungeanum based on human sensation. J Sens Stud. 2018;33(6):e12465.

[4] Zeng M, Wang J, Zhang M, Chen J, He Z, Qin F, et al. Inhibitory effects of Sichuan pepper (Zanthoxylum bungeanum) and sanshoamide extract on heterocyclic amine formation in grilled ground beef patties. Food Chem. 2018;239:111–8.

[5] Li K, Zhou R, Wang Jia W, Li Z, Li J, Zhang P, et al. Zanthoxylum bungeanum essential oil induces apoptosis of HaCaT human keratinocytes. J Ethnopharmacol. 2016;186:351–61.

[6] Fu L, Liu Z, Ge J, Guo M, Zhang H, Chen F, et al. (001) plan manipulation of α-Fe_2O_3 nanostructures for enhanced electrochemical Cr(VI) sensing. J Electroanal Chem. 2019;841:142–7.

[7] Yu J, Jin H, Gui R, Lv W, Wang Z. A facile strategy for ratiometric electrochemical sensing of quercetin in electrolyte solution directly using bare glassy carbon electrode. J Electroanal Chem. 2017;795:97–102.

[8] Xu Y, Lu Y, Zhang P, Wang Y, Zheng Y, Fu L, et al. Infrageneric phylogenetics investigation of Chimonanthus based on electroactive compound profiles. Bioelectrochemistry. 2020;133:107455.

[9] Yang L, Xu B, Ye H, Zhao F, Zeng B. A novel quercetin electrochemical sensor based on molecularly imprinted poly(para-aminobenzoic acid) on 3D Pd nanoparticles-porous graphene-carbon nanotubes composite. Sens Actuators B Chem. 2017;251:601–8.

[10] Fu L, Zheng Y, Zhang P, Zhang H, Xu Y, Zhou J, et al. Development of an electrochemical biosensor for phylogenetic analysis of Amaryllidaceae based on the enhanced electrochemical fingerprint recorded from plant tissue. Biosens Bioelectron. 2020;159:112212.

[11] Vilian ATE, Puthiaraj P, Kwak CH, Choe SR, Huh YS, Ahn W-S, et al. Electrochemical determination of quercetin based on porous aromatic frameworks supported Au nanoparticles. Electrochim Acta. 2016;216:181–7.

[12] Zhou J, Zheng Y, Zhang J, Karimi-Maleh H, Xu Y, Zhou Q, et al. Characterization of the electrochemical profiles of lycoris seeds for species identification and infrageneric relationships. Anal Lett. 2020;53(15):2517–28.

[13] Takahashi S, Muguruma H, Osakabe N, Inoue H, Ohsawa T. Electrochemical determination with a long-length carbon nanotube electrode of quercetin glucosides in onion, apple peel, and tartary buckwheat. Food Chem. 2019;300:125189.

[14] Yao Z, Yang X, Liu X, Yang Y, Hu Y, Zhao Z. Electrochemical quercetin sensor based on a nanocomposite consisting of magnetized reduced graphene oxide, silver nanoparticles and a molecularly imprinted polymer on a screen-printed electrode. Microchim Acta. 2017;185(1):70.

[15] Gomez FJV, Espino M, de los Angeles Fernandez M, Raba J, Silva MF. Enhanced electrochemical detection of quercetin by natural deep eutectic solvents. Anal Chim Acta. 2016;936:91–6.

[16] Zhang W, Zong L, Geng G, Li Y, Zhang Y. Enhancing determination of quercetin in honey samples through electrochemical sensors based on highly porous polypyrrole coupled with nanohybrid modified GCE. Sens Actuators B Chem. 2018;257:1099–109.

[17] Liu J, Li X, Weng W, Xie H, Luo G, Niu Y, et al. A biomass-derived porous carbon-based nanocomposite for voltammetric determination of quercetin. Microchim Acta. 2019;186(12):783.

[18] Zhao P, Ni M, Xu Y, Wang C, Chen C, Zhang X, et al. A novel ultrasensitive electrochemical quercetin sensor based on MoS_2 – carbon nanotube @ graphene oxide nanoribbons/HS-cyclodextrin/graphene quantum dots composite film. Sens Actuators B Chem. 2019;299:126997.

[19] Li J, Qu J, Yang R, Qu L, de B, Harrington P. A sensitive and selective electrochemical sensor based on graphene quantum dot/gold nanoparticle nanocomposite modified electrode for the determination of quercetin in biological samples. Electroanalysis. 2016;28(6):1322–30.

[20] Khodarahmi R, Khateri S, Adibi H, Nasirian V, Hedayati M, Faramarzi E, et al. Chemometrical-electrochemical investigation for comparing inhibitory effects of quercetin and its sulfonamide derivative on human carbonic anhydrase II: Theoretical and experimental evidence. Int J Biol Macromol. 2019;136:377–85.

[21] Alipour F, Raoof JB, Ghani M. Determination of quercetin via thin film microextraction using the *in situ* growth of Co–Al-layered double hydroxide nanosheets on an electrochemically anodized aluminum substrate followed by HPLC. Anal Methods. 2020;12(6):799–806.

[22] Krukiewicz K, Gniazdowska B, Jarosz T, Herman AP, Boncel S, Turczyn R. Effect of immobilization and release of ciprofloxacin and quercetin on electrochemical properties of poly(3,4-ethylenedioxypyrrole) matrix. Synth Met. 2019;249:52–62.

[23] Zhang X, Yang R, Li Z, Zhang M, Wang Q, Xu Y, et al. Electroanalytical study of infrageneric relationship of Lagerstroemia using glassy carbon electrode recorded voltammograms. Revista Mexicana de Ingeniería Química. 2020;19(Supp. 1):281–91.

[24] Abdel-Hamid R, Rabia MK, Newair EF. Electrochemical behaviour of antioxidants: part 2. Electrochemical oxidation mechanism of quercetin at glassy carbon electrode modified with multi-wall carbon nanotubes. Arab J Chem. 2016;9(3):350–6.

[25] Demir E, Senocak A, Tassembedo-Koubangoye MF, Demirbas E, Aboul-Enein HY. Electrochemical evaluation of the total antioxidant capacity of yam food samples on a poly-glycine-glassy carbon modified electrode. Curr Anal Chem. 2020 Mar 1;16(2):176–83.

[26] Chen Y, Huang W, Chen K, Zhang T, Wang Y, Wang J. Facile fabrication of electrochemical sensor based on novel core-shell PPy@ZIF-8 structures: enhanced charge collection for quercetin in human plasma samples. Sens Actuators B Chem. 2019;290:434–42.
[27] Zhang M, Pan B, Wang Y, Du X, Fu L, Zheng Y, et al. Recording the electrochemical profile of pueraria leaves for polyphyly analysis. ChemistrySelect. 2020;5(17):5035–40.
[28] Niu X, Li X, Chen W, Li X, Weng W, Yin C, et al. Three-dimensional reduced graphene oxide aerogel modified electrode for the sensitive quercetin sensing and its application. Mater Sci Eng C. 2018;89:230–6.
[29] Veerakumar P, Rajkumar C, Chen S-M, Thirumalraj B, Lin K-C. Ultrathin 2D graphitic carbon nitride nanosheets decorated with silver nanoparticles for electrochemical sensing of quercetin. J Electroanal Chem. 2018;826:207–16.
[30] He R-X, Zha D-W. Cyclic voltammetry and voltabsorptometry studies of redox mechanism of lumazine. J Electroanal Chem. 2017;791:103–8.
[31] Catauro M, Bollino F, Nocera P, Piccolella S, Pacifico S. Entrapping quercetin in silica/polyethylene glycol hybrid materials: chemical characterization and biocompatibility. Mater Sci Eng C. 2016;68:205–12.
[32] Diamantis DA, Ramesova S, Chatzigiannis CM, Degano I, Gerogianni PS, Karadima KE, et al. Exploring the oxidation and iron binding profile of a cyclodextrin encapsulated quercetin complex unveiled a controlled complex dissociation through a chemical stimulus. Biochim Biophys Acta BBA Gen Subj. 2018;1862(9):1913–24.
[33] Kocábová J, Fiedler J, Degano I, Sokolová R. Oxidation mechanism of flavanone taxifolin. Electrochemical and spectroelectrochemical investigation. Electrochim Acta. 2016;187:358–63.
[34] Sokolová R, Tarábek J, Papoušková B, Kocábová J, Fiedler J, Vacek J, et al. Oxidation of the flavonolignan silybin. *In situ* EPR evidence of the spin-trapped silybin radical. Electrochim Acta. 2016;205:118–23.
[35] Heřmánková E, Zatloukalová M, Biler M, Sokolová R, Bancířová M, Tzakos AG, et al. Redox properties of individual quercetin moieties. Free Radic Biol Med. 2019;143:240–51.
[36] Ramešová Š, Degano I, Sokolová R. The oxidative decomposition of natural bioactive compound rhamnetin. J Electroanal Chem. 2017;788:125–30.
[37] Al Haddabi B, Al Lawati HAJ, Suliman FO. A comprehensive evaluation of three microfluidic chemiluminescence methods for the determination of the total phenolic contents in fruit juices. Food Chem. 2017;214:670–7.
[38] Patra M, Mukherjee R, Banik M, Dutta D, Begum NA, Basu T. Calcium phosphate-quercetin nanocomposite (CPQN): a multifunctional nanoparticle having pH indicating, highly fluorescent and anti-oxidant properties. Colloids Surf B Biointerfaces. 2017;154:63–73.
[39] Lynk TP, Clarke OJR, Kesavan N, Brosseau CL. Development of a sustainable plasmon-enhanced spectroelectrochemical sensor using avocado pit (Persea americana) extract. Sens Actuators B Chem. 2018;257:270–7.
[40] Revenga-Parra M, Robledo SN, Martínez-Periñán E, González-Quirós MM, Colina A, Heras A, et al. Direct determination of monosaccharides in honey by coupling a sensitive new Schiff base Ni complex electrochemical sensor and chemometric tools. Sens Actuators B Chem. 2020;312:127848.
[41] Ipte PR, Kumar S, Satpati AK. Electrochemical synthesis of carbon nano spheres and its application for detection of ciprofloxacin. J Environ Sci Health Part A. 2020;55(2):142–50.
[42] Tang J, Mao Y, Guo J, Li Z, Zhang C, Jin B. Simultaneous determination of TBH2Q and BHA Antioxidants in food samples using Eosin Y Film modified electrode. Food Anal Methods. 2018;11(12):3380–90.
[43] Zhiltsova EP, Ibatullina MR, Lukashenko SS, Kutyreva MP. Zakharova LYa. Spectrophotometric study of quercetin in metallomicellar solutions of 1-hexadecyl-4-aza-1-azoniabicyclo[2.2.2]octane bromide complex with copper dibromide. J Mol Liq. 2018;249:716–22.
[44] Vinnarasi S, Radhika R, Vijayakumar S, Shankar R. Structural insights into the anti-cancer activity of quercetin on G-tetrad, mixed G-tetrad, and G-quadruplex DNA using quantum chemical and molecular dynamics simulations. J Biomol Struct Dyn. 2020;38(2):317–39.
[45] Zagrean-Tuza C, Dorneanu S, Mot AC. The strange case of polyphenols inhibiting the Briggs-Rauscher reaction: pH-modulated reactivity of the superoxide radical. Free Radic Biol Med. 2020;146:189–97.
[46] Jalalvand AR, Goicoechea HC. Applications of electrochemical data analysis by multivariate curve resolution-alternating least squares. Trends Anal Chem. 2017;88:134–66.
[47] Klein E, Rimarčík J, Senajová E, Vagánek A, Lengyel J. Deprotonation of flavonoids severely alters the thermodynamics of the hydrogen atom transfer. Comput Theor Chem. 2016;1085:7–17.
[48] Gulsunoglu Z, Purves R, Karbancioglu-Guler F, Kilic-Akyilmaz M. Enhancement of phenolic antioxidants in industrial apple waste by fermentation with Aspergillus spp. Biocatal Agric Biotechnol. 2020;71:101562.
[49] Yang S-L, Zhao L-J, Chi S-M, Du J-J, Ruan Q, Xiao P-L, et al. Inclusion complexes of flavonoids with propylenediamine modified β-cyclodextrin: preparation, characterization and antioxidant. J Mol Struct. 2019;1183:118–25.
[50] Waffo AFT, Yesildag C, Caserta G, Katz S, Zebger I, Lensen MC, et al. Fully electrochemical MIP sensor for artemisinin. Sens Actuators B Chem. 2018;275:163–73.
[51] Sahoo S, Sahoo PK, Sharma A, Satpati AK. Interfacial polymerized RGO/$MnFe_2O_4$/polyaniline fibrous nanocomposite supported glassy carbon electrode for selective and ultrasensitive detection of nitrite. Sens Actuators B Chem. 2020;309:127763.
[52] Brinkert K, Le Formal F, Li X, Durrant J, Rutherford AW, Fantuzzi A. Photocurrents from photosystem II in a metal oxide hybrid system: electron transfer pathways. Biochim Biophys Acta BBA Bioenerg. 2016;1857(9):1497–505.
[53] Ramos II, Gregório BJR, Barreiros L, Magalhães LM, Tóth IV, Reis S, et al. Programmable flow system for automation of oxygen radical absorbance capacity assay using pyrogallol red for estimation of antioxidant reactivity. Talanta. 2016;150:599–606.
[54] Chernikov DA, Shishlyannikova TA, Kashevskii AV, Bazhenov BN, Kuzmin AV, Gorshkov AG, et al. Some peculiarities of taxifolin electrooxidation in the aqueous media: the dimers formation as a key to the mechanism understanding. Electrochim Acta. 2018;271:560–6.